

BBAMEM 74710

## Alterations in the electrical properties of T and B lymphocyte membranes induced by mitogenic stimulation. Activation monitored by electro-rotation of single cells

Xun Hu \*, W. Michael Arnold and Ulrich Zimmermann

*Lehrstuhl für Biotechnologie der Universität Würzburg, Würzburg (F.R.G.)*

(Received 26 July 1989)

**Key words:** Concanavalin A; Lipopolysaccharide; Agglutinin, peanut; Membrane capacity; Membrane conductivity; Surface conductance; Electrorotation

Stimulation of either B or T lymphocytes using specific mitogens results in changes in the passive electrical properties of the cell surface. These effects can be related to growth and secretion. This was possible because the high resolution of the contra-field electro-rotation method, combined with the use of very low conductivity media, allowed accurate and analytically-derived values for the cell surface properties. Increases in effective  $C_M$  (membrane capacity) and changes in apparent membrane conductivity (reflecting the additive effects of true membrane conductivity  $G_M$  and surface conductance  $K_S$ ) were measured. After 72 h treatment with concanavalin A, thymocyte  $C_M$  had increased from  $0.76 \mu\text{F}/\text{cm}^2$  to  $1.24\text{--}1.46 \mu\text{F}/\text{cm}^2$  ( $7.6$  to  $12.4\text{--}14.6 \text{ mF}/\text{m}^2$ ). Allowing for the stimulation-induced size increase (cell radius increased from  $2.8$  to  $4.4 \mu\text{m}$ ) these data imply that the plasma membrane area per cell increases 5-fold during stimulation. Stimulation of B cells (by 3 days incubation with bacterial lipopolysaccharide) increased  $C_M$  from  $0.93$  to  $1.6\text{--}1.7 \mu\text{F}/\text{cm}^2$  ( $9.3$  to  $16\text{--}17 \text{ mF}/\text{m}^2$ ). Incubation without mitogen gave no significant increase in  $C_M$  or in radius. Control cells of different sizes showed no difference in membrane properties. The increases in effective  $C_M$  are argued to reflect an increase in membrane ramification (microvilli, folding, etc.). The apparent membrane conductivity of T cells also increased during stimulation, from  $5$  to  $21 \text{ mS}/\text{cm}^2$  ( $50$  to  $210 \text{ S}/\text{m}^2$ ). This increase is proportionately much greater than that in  $C_M$  or in membrane area. It seems to be due to a real increase in  $G_M$ , but a small increase in  $K_S$  may also occur. The earliest changes in apparent membrane conductivity were evident between 3 and 5 h after stimulation, before the cells increased in size. This response parallels increases in transmembrane transport reported to follow mitogenic stimulation.

### Introduction

It has been recognised since 1968 that there are two functionally distinct types of lymphocyte: B cells (derived from bone marrow) produce antibodies, whereas T cells (from the thymus) are responsible for cytotoxicity, delayed type hypersensitivity and the regulation of many B and T cell functions. Although in vivo expression of these functions is dependent upon the presence

of many cell types, in vitro expression of certain functions may be induced with mitogens which are specific to cell type [1].

Despite extensive studies of morphology, immunology and biochemistry, comparison of the electrical properties of the two types of lymphocytes and of their stimulated forms has been limited to electrophoresis [2–4] and membrane potential [5]. Studies at higher frequencies have been more restricted in method and in choice of material. Thymocytes have been measured [6] by the suspension impedance technique, but not by the other high-frequency technique, dielectrophoretic collection [7,8]. Both of these suspension methods average over large numbers of cells and therefore cannot differentiate between the properties of unstimulated and stimulated cells in a mixed population.

The method of choice for activation studies would appear to be single-cell rotation. This has been used on a large variety of cells [9–14], even when these are only available in small quantities. Analytical solutions for

\* Permanent address: Cancer Institute of the Zhejiang Medical University, Hangzhou, Zhejiang Province, China.

Abbreviations: Con A, concanavalin A; FCS, foetal calf serum; LPS, bacterial lipopolysaccharide; PBS, phosphate-buffered saline; PNA, peanut (*Arachis hypogaea*) agglutinin; SBA, soybean (*Glycine max*) agglutinin.

Correspondence: W.M. Arnold, Lehrstuhl für Biotechnologie der Universität Würzburg, Röntgenring 11, D-87 Würzburg, F.R.G.

the surface properties are practical [9,15]. Earlier work [16] showed that a distinction between inactive and antibody-secreting lymphocytes was possible using electro-rotation, and differences between mixed peripheral blood lymphocytes and those stimulated with Con A have also been seen [17]. However no analytically-derived data on the membrane properties was available. The high resolution of analytically-derived data allows derivation of data on surface architecture and membrane transport.

## Materials and Methods

### (a) Cells

Animals were 6–10-weeks old male Balb/c mice. Immediately after killing an animal, either spleen and lymph node cells or else thymocytes were prepared as below.

The spleen and the mesenteric lymph node were removed from the peritoneal cavity, or else both lobes of the thymus were removed from the thoracic cavity. Erythrocytes were washed away in PBS, and the organ(s) teased gently apart in PBS until a suspension was obtained that could be filtered through a stainless steel gauze to give a cellular suspension.

In the case of spleen or lymph node cells, separation of B cells from T cells used the following modifications of the procedures of Reisner et al. [18]. Agglutination of splenic B cells occurred during 10-min incubation with 1 mg/ml SBA. The mixture was layered onto 20 ml medium (80% PBS and 20% heat-inactivated FCS). After 30 min the agglutinated B cells had sedimented out of the upper half of the tube. The agglutinated cells were dispersed by 10-min incubation in 0.2 M galactose in PBS, followed by two washes with this medium. In the case of thymic cells, agglutination of immature thymocytes enabled their separation [19]. Incubation was at  $1 \cdot 10^7$  cells/ml with 1 mg/ml PNA for 10 min at 20°C. After 30 min settling through 20 ml medium (as above) the two fractions (agglutinated immature cells in the pellet, dispersed mature cells in the supernate) were each washed twice with 0.2 M galactose in PBS.

### (b) Stimulation

Mixed lymphocyte suspensions were stimulated either with LPS (10 µg/ml of Sigma L-2880) or Con A (5 µg/ml of Sigma L-2769); only the latter was used for thymocytes. These mitogens give specific stimulation of B or of T cells, respectively [1]. Incubation was for stated periods in RPMI-1640 (+10% FCS) at 37°C in a CO<sub>2</sub> incubator.

### (c) Rotation technique

Before use all cells were washed twice with 320 mM glucose (conductivity 2 µS/cm) and the conductivity adjusted with 1 mM KCl to the desired value for

electro-rotation (3–5 µS/cm, 8–10 µS/cm, 13–15 µS/cm or 19–20 µS/cm). Microscopic observation of cells in these media showed that they had the same 'hairy' morphology as seen in growth medium (the cell surface appears to be covered with fine hairs). However, after prolonged incubation in glucose media (more than 20 min) a few cells had a featureless and highly transparent membrane, and were usually larger than the 'hairy' cells. Data on these cells was noted separately. In a few experiments inositol was substituted for glucose. The rotational results were identical although no 'transparent' cells were produced.

We tested for damage by low-ionic media (at 4.4 µS/cm conductivity) by counting those cells permeable to a fluorescent nuclear stain, propidium iodide. Increase of the incubation time from 10 to 50 min increased the fraction of permeable cells in inositol from 5% to 7.5%, and in glucose from 8% to 10%. Incubations in culture medium (RPMI 1640) were only slightly better (stained cells increased from 5% to 7% over the same period). We conclude that the rotation media did not damage significant numbers of cells within the time required for measurement (20–30 minutes).

The rotation chamber had inner dimensions of a cube of side 1.5 mm, with platinum electrodes occupying 67% of each side. The top of the chamber was open to allow rapid exchange of cell suspension. The chamber floor, a removable cover-glass of 0.15 mm thickness, permitted the use of high-resolution optics (100× oil-immersion objective fitted to a Leitz Labovert modified for interference contrast). Conductivity within the chamber was monitored between individual measurements by the automatic connection of a conductometer to two opposite electrodes.

For each cell the diameter was measured whilst the field frequency that gave fastest anti-field rotation (the  $f_c$ ) was determined. This frequency is directly connected with the charging time of the membrane, so that membrane capacity and conductivity may be deduced as explained below. Use of the contra-rotating field technique [20,21] allowed  $f_c$  measurements on 50 cells in 20 min. In some cases measurements of the rotation speed at the  $f_c$  were also carried out (by timing 10 revolutions with a stop-watch). Rotation spectra were taken with the apparatus described in Ref. 9.

### (d) The form of the rotation spectrum

Electro-rotation is a method of examining the electrical properties of single particles by means of a rotating electrical field [9,14,15]. The field induces a rotating dipole within the particle: the dipole may rotate ahead of or behind the field in the medium. The angle between dipole and field results in a torque on the cell, which leads to particle rotation at rates up to a few Hz. The particle speed is not directly connected with the rate of field rotation: rotation spectra such as shown in Fig. 1

are a means of testing whether the phenomenon agrees with theory.

In low-conductivity media such as used for Fig. 1, kHz frequencies of rotating field give rise to anti-field rotation (opposite to the sense of the field). This rotation is due to a dipole associated with the field-induced plasma membrane voltage. If the charging time of the plasmamembrane is  $\tau$ , then the field frequency that gives maximum anti-field rotation ( $f_c$ ) is given by  $2\pi f_c = 1/\tau$  [9,14,15,22,23]. When an internal membrane system also exerts an effect on the rotation (e.g., the tonoplast in mesophyll protoplasts [9,24]), the spectra are more complex (broadened, or with a 'shoulder') than in Fig. 1 are measured. In addition, measurements over a range of conductivities cannot be described by the linear form of Eqn. 1 below [9]. However, the experimental points in Fig. 1 agree very well with the theoretical expression [9,15,22] derived for a single membrane-charging process (the continuous curves in Fig. 1), and Eqn. 1 fits the data very well over a 7:1 range of conductivities (see Fig. 2 below).

Both of the above tests of the data show that, at the medium conductivities used here, the equations given in the next section can be used to derive values for the surface parameters of the cell, independent of membranes other than the plasma membrane.

It has been reported [17] that some peripheral blood lymphocytes from mice show spectra in which the anti-field rotation peak is not symmetrical as in Fig. 1, but asymmetrical because of the large size of the nucleus. In none of the rotation spectra which we examined was such asymmetry apparent. The reason that the lymphocyte spectra in Ref. 17 are more complex and variable than ours may be that they were taken in medium conductivities of 250  $\mu\text{S}/\text{cm}$  instead of the 30  $\mu\text{S}/\text{cm}$  in Fig. 1\*. Assuming this to be the case, we carried out all our further measurements at still lower conductivities of 5–20  $\mu\text{S}/\text{cm}$ . A further difference is that peripheral cells from human blood were used in Ref. 17, not lymph node, spleen or thymus cells from mice. One or more of these differences presumably accounts for the observation that although the rotational mobility of the cells examined in Ref. 17 was in the range  $-(0.8\text{--}1.3) \cdot 10^{-4} \text{ rev} \cdot \text{cm}^2 \cdot \text{s}^{-1} \cdot \text{V}^{-2}$ , our data (Fig. 1 and Table I) are in the range  $-(1.9\text{--}2.3) \cdot 10^{-4} \text{ rev} \cdot \text{cm}^2 \cdot \text{s}^{-1} \cdot \text{V}^{-2}$ .

A last point supporting the neglect of the nuclear

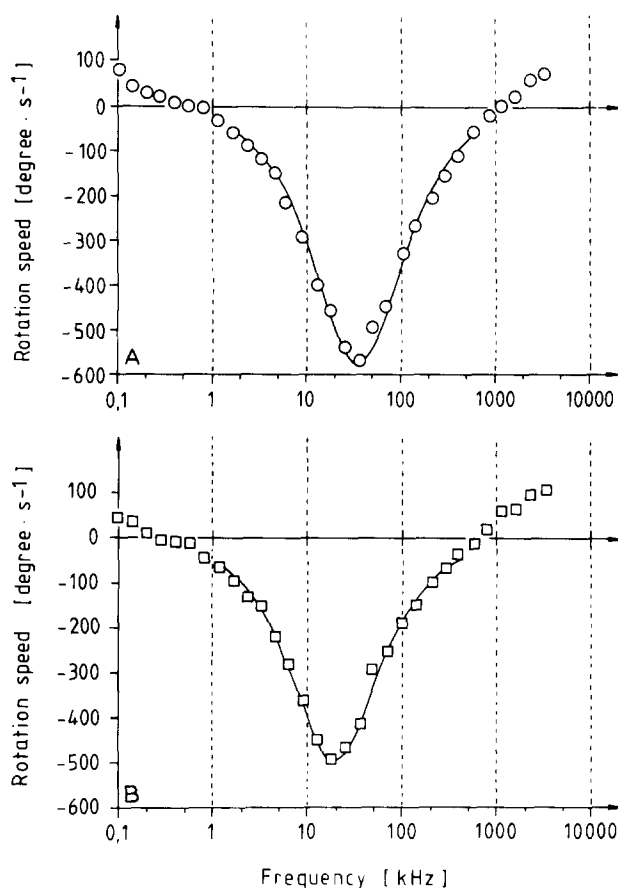


Fig. 1. Rotation spectra of 72-h control-incubated (A, '○' symbols) and of 72-h Con-A-stimulated (B, '□' symbols) thymocytes in medium of 30  $\mu\text{S}/\text{cm}$  conductivity. In each case, several cells were measured at a constant field strength of 82 V/cm, using a frequency-stepper and video apparatus [9]. Two cells with closely-similar radius and peak-frequency ( $f_c$ ) were selected in each case, and the means at each frequency gave the displayed data. The deviations of the speeds within each cell pair were 10% or less at all frequencies. The continuous curves are plots of the function  $\Omega = \Omega_0 \cdot 2F/(1 + F^2)$ , a general function for a rotation peak where only a single time-constant is effective (for example when only a single membrane-charging process dominates the spectrum). Here  $F$  is the normalised field frequency ( $f/f_c$ ) and  $\Omega_0$  is the maximum rotation speed. The amplitude  $\Omega_0$  and  $f_c$  are taken from experimental measurements at  $f_c$ . The good agreement of the experimental frequency-dependence with theory allows us to conclude that our data can be interpreted in terms of a single membrane. The two control cells had  $f_c$  of  $32 \pm 0.3$  kHz, the stimulated cells  $f_c$  of  $19 \pm 0.4$  kHz. In these two cases the rotational mobilities can be calculated to be  $-2.3 \cdot 10^{-4} \text{ rev} \cdot \text{cm}^2 \cdot \text{s}^{-1} \cdot \text{V}^{-2}$  and  $-2.0 \cdot 10^{-4} \text{ rev} \cdot \text{cm}^2 \cdot \text{s}^{-1} \cdot \text{V}^{-2}$ , respectively (see Table I for values meaned over a larger sample).

membrane in this work is the very high conductance of this membrane in mouse lymphocytes [6] (see Discussion).

Fig. 1 is the first published spectrum which shows that, at sufficiently low frequencies, co-field rotation of cells can occur. A similar effect has been reported for polystyrene particles [25], and is also exhibited by chloroplasts, by yeast protoplasts and by some erythrocytes (Arnold, W.M. and Zimmermann, U., unpub-

\* This point is argued elsewhere [9] in relation to the tonoplast/plasma membrane problem in plant protoplasts. The essential point is that use of higher medium conductivities shifts the entire anti-field rotation peak to higher frequencies. At low frequencies the inner membrane passes so little current that it has little effect on the rotation, but at higher frequencies the rotation depends on both membrane systems. The method of using a very low conductivity also enabled the plasma membrane of protoplasts to be measured independently from the tonoplast [9].

TABLE I

Rotation speeds of stimulated and control lymphocytes

Thymocytes were incubated for three days with or without Con A and then prepared for rotation. After individual adjustment of the field frequency to the  $f_c$ , the rotation speed of each cell was measured by timing six revolutions with a stopwatch. The results are means and standard deviations of the indicated numbers of cells ( $n$ ). The field strength was 48.0 V/cm, so that the mean speed of close to 0.44 antifield revolution/s corresponds to a rotational mobility of  $-1.9 \cdot 10^{-4} \text{ rev} \cdot \text{cm}^2 \cdot \text{s}^{-1} \cdot \text{V}^{-2}$ .

	Cell radius ( $\mu\text{m}$ )	Rotation speed (revolution/s) in media of conductivity:	
		$11 \pm 2 \mu\text{S/cm}$	$22 \pm 2.5 \mu\text{S/cm}$
Control	$3.1 \pm 0.3$ ( $n = 34$ )	$0.4 \pm 0.09$ ( $n = 20$ )	$0.46 \pm 0.04$ ( $n = 14$ )
Stimulated	$4.1 \pm 0.4$ ( $n = 27$ )	$0.44 \pm 0.07$ ( $n = 17$ )	$0.43 \pm 0.03$ ( $n = 10$ )

lished data). This effect is not covered by existing theoretical work, although it has been suggested that it is probably due to modification of the field seen by the particle by the dielectric response of the ionic double layer [25]. This weak co-field response is not expected to affect deductions made from the anti-field peak, because this is much stronger and occurs at frequencies some 100-times higher.

(e) Derivation of membrane parameters from rotation data

We have found that the most useful approach to electrorotation measurements is to measure the  $f_c$  in a series of media of different conductivities ( $\sigma_1$ , in S/cm). The aim is to derive information on the surface properties of the cell. The most useful properties are membrane capacity  $C_M$ , in  $\mu\text{F/cm}^2$ ; membrane conductivity  $G_M$ , in  $\text{mS/cm}^2$ ; in the case of cells as small as lymphocytes  $G_M$  is difficult to separate from the surface conductance  $K_S$ , in S (the meaning of  $K_S$  is discussed below). To the extent that the surface of many biological cells is structured, whereas these parameters are based on smooth spherical models, all data must be accepted as 'effective' values. The effective  $C_M$  is a particularly useful parameter for characterising the sum of changes in surface structure and composition.

If the radius ( $a$ , in cm) of each cell is measured, the following equation can be applied in order to derive cell surface data [9]:

$$f_c \cdot a = \frac{K_s}{\pi \cdot a \cdot C_M} + \frac{a \cdot G_M}{2\pi \cdot C_M} + \frac{\sigma_1}{\pi \cdot C_M} \quad (1)$$

The use of this relationship is restricted to values of  $\sigma_1$  that are much lower than the internal conductivity of the cell. If the medium conductivity is increased too much,  $f_c$  no longer increases linearly with  $\sigma_1$  and the cell rotation rate decreases [15]. However, measure-

ments of rotation speed (Table I) show the rotation rate to be independent of conductivity in the range used.

The degree of linearity of a plot of  $f_c \cdot a$  with respect to  $\sigma_1$  provides a basis for confirming whether the assumptions required for Eqn. 1 are justified. Such a plot is also a means for the rapid display and assessment (using the correlation coefficient  $r$  of a least-squares fit) of rotation data, such as in Fig. 2. It is possible to plot each cell measurement (Fig. 2A) or to plot the means of 8–12 measurements taken at closely similar  $\sigma_1$  (Fig. 2B). The latter procedure forfeits the single-cell resolution of the data but provides a better test of the

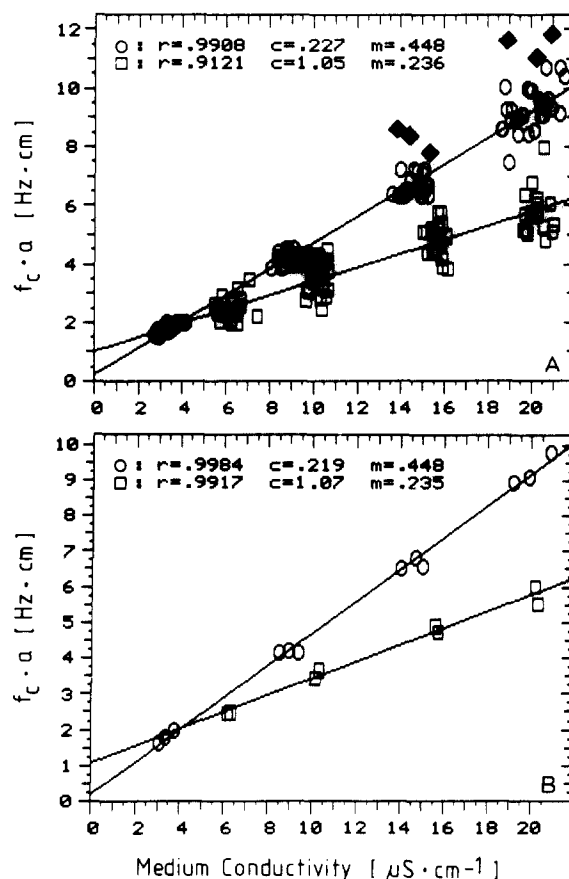


Fig. 2. Specimen rotation data on unstimulated thymocytes ( $\circ$ ) and on thymocytes that had been stimulated for 72 h with Con A ( $\square$ ). The  $\blacklozenge$  symbols show six unstimulated cells that were of altered appearance, probably due to extended incubation in low-ionic medium. These cells were not included in further analysis. The frequency giving fastest rotation ( $f_c$ ), the cell radius ( $a$ ), and the medium conductivity within the chamber were recorded for each cell. In (A), each cell is represented by one symbol, which gives rise to considerable overlapping (112 unstimulated and 83 stimulated cells were measured in this example). By taking means of 8–12 cells measured at closely similar conductivities, the presentation of the data is made clearer (B). Standard deviations of the conductivities were 4–5% (at 3–7  $\mu\text{S/cm}$ ) and 1–2% (at 14–21  $\mu\text{S/cm}$ ) of the means, standard deviations of the  $f_c \cdot a$  values are in the range 2.8–7.5% (controls) or 8.2–16.9% (Con A-treated) of the means. The surface parameters  $C_M$  and  $G_A$  are obtained from the slope and intercept of the regression lines (see Eqn. 1).

linearity of the relationship between  $f_c \cdot a$  and  $\sigma_1$ . Note that the correlation coefficients ( $r$  in Fig. 2) on the mean data are better than on the single-cell data, because the latter are more affected by cell variability. Provided that sufficient measurements are made at each conductivity, linear regressions on either data set provide values for the gradient ( $m$ ) and intercept ( $c$ ) which are the same or nearly so. The mean data demonstrates particularly effectively that Eqn. 1 fits these data well.

In both parts of Fig. 2, circles represent untreated thymocytes, whereas squares represent thymocytes that had been stimulated with Con A for 72 h. The six filled diamonds in Fig. 2A represent control thymocytes that had the altered appearance ('transparent') referred to in the Methods: these cells were not included in the mean values or regression analyses. The gradients ( $m$  values in Fig. 2) of such linear regressions are estimates of  $1/\pi C_M$ . The normalisation of  $f_c$  against  $a$  in Eqn. 1 allows  $C_M$  values of cells of different sizes to be compared directly in Fig. 2. It is readily seen that the  $C_M$  of the stimulated cells is almost double that of the untreated cells.

#### (f) Surface conductance and membrane conductivity

Eqn. 1 shows that not only membrane capacity  $C_M$  but also the surface conductance  $K_S$  and membrane conductivity  $G_M$  affect the  $f_c$ . These conductance parameters may exert comparable effects on the total cellular conductance [15]: one way to separate their effects is by observations on cells of different sizes [9].

The  $K_S$  of a particle is the tangential conductance through a surface layer of enhanced conductivity (Fig. 3), ideally of zero thickness. Practical examples are the counter-ion layers to surface charges or the counter ions within the glycocalix (or cell wall). Fig. 3 shows how the total current that flows from one side of the cell to the other is the sum of the current flowing through this surface layer and the current through the membrane. Comparison of electrophoretic mobility (which reflects net surface charge) with electro-rotation  $K_S$  may be possible. An increase of net negative surface charge will increase the number of positive counter-ions in the surface layer and therefore tend to increase  $K_S$ .

The intercept on the  $f_c \cdot a$  axis of plots such as Fig. 2 gives information on the *sum* of the effects of  $G_M$  and  $K_S$ . This intercept may be divided by the radius of the class of cells measured to give a theoretical value for  $f_c$  at zero  $\sigma_1$ . We term this  $f_{c0}$ :

$$f_{c0} = \frac{G_A}{2\pi \cdot C_M} \quad (2)$$

where  $G_A$  is the apparent membrane conductivity and includes the radius-dependent effect of  $K_S$ :

$$G_A = G_M + (2K_S/a^2) \quad (3)$$

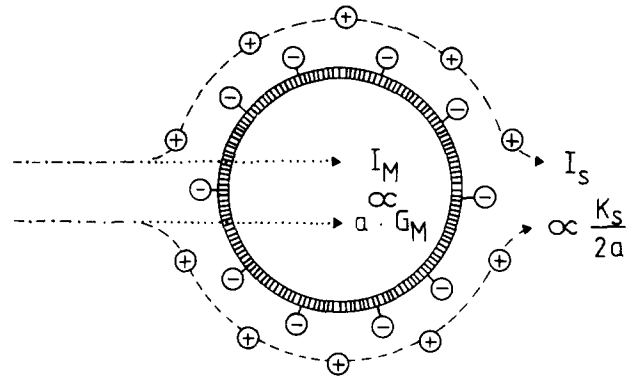


Fig. 3. Diagram of a cell to illustrate the concept of surface conductance ( $K_S$ ), an important electrical parameter for small cells in low-conductive media. The lines represent current flow in response to an external field. The conductive (as opposed to capacitive) current is not only the current that flows through the membrane ( $I_M$ , proportional to membrane conductivity  $G_M$ ) but has also a component  $I_S$  that flows in a layer close to the cell surface. The conductivity of this layer is enhanced by the counterions ('+') to the surface charge ('-') on the membrane and glycocalix. This layer is assumed to be thin compared to the cell radius, so that it acts as a 'surface' conductance  $K_S$ . Geometrical arguments [9] show that  $I_M$  increases with cell radius (as  $a \cdot G_M$ ), whereas  $I_S$  decreases with cell radius (as  $K_S/2a$ ). Therefore the importance of  $K_S$  relative to  $G_M$  increases rapidly as the radius decreases (see Eqn. 3).

This equation shows that unambiguous interpretation of  $G_M$  values from electro-rotation is only possible when the cell is large enough to reduce the effect of  $K_S$  sufficiently. Thus rotation of oocytes ( $a = 54 \mu\text{m}$ ) allowed measurement of  $G_M$  values of 1–14 mS/cm<sup>2</sup> [11]. However, if such values are measured on lymphocytes, no certain value can be given to  $G_M$ . This is because  $K_S$  contributions to  $G_A$  of 5.1 to 53 mS/cm<sup>2</sup> would be expected from Eqn. 3 for cells of the size of unstimulated lymphocytes ( $a = 2.8 \mu\text{m}$ ), assuming that the  $K_S$  of cells are within the range 0.2 to 2.1 nS, values measured on insulating particles [25].

## Results

### (a) Control T and B cells

Freshly-prepared lymphocytes exhibited membrane capacities of 0.7–0.8  $\mu\text{F}/\text{cm}^2$  (T cells) or 0.9  $\mu\text{F}/\text{cm}^2$  (B cells), see Table II. In the case of T cells, no difference could be detected between the membrane capacities of cells of different sizes (2.5–3.1  $\mu\text{m}$ ) or between the sub-groups of immature and mature cells separated by selective agglutination with PNA. PNA-negative (mature) cells showed an apparent membrane conductivity ( $G_A$ ) that was usually higher than that of PNA-agglutinatable (immature) cells. The values of  $G_A$  of small (2.5  $\mu\text{m}$  and 2.8  $\mu\text{m}$  radius) unstimulated T cells are 4.7 mS/cm<sup>2</sup> and 5.5 mS/cm<sup>2</sup>, respectively. Substitution into Eqn. 3 yields  $K_S$  values of 0.15 nS and 0.22 nS, respectively (maximum values, assuming  $G_M = 0$ ). These

TABLE II

The membrane capacity ( $C_M$ ) and apparent conductivity ( $G_A$ ) of fresh, unstimulated T and B cells

Three groups of data are shown: (1) Untreated T cells were measured and the data classified according to cell radius ( $a$ ,  $\mu\text{m}$ ); (2) Immature and mature sub-fractions of the T cell population were separated with peanut agglutinin (PNA); (3) B lymphocytes were purified from spleen cells by use of soybean agglutinin (SBA). Most data are means  $\pm$  S.D. from five determinations, except for those in the first column which are the means and deviations of just two. In each determination 40–50 cells of each group were measured.

	T cells of radius $a$ ( $\mu\text{m}$ )			T cells ( $a = 2.8 \mu\text{m}$ )		B cells ( $a = 2.8 \mu\text{m}$ )
	$a = 2.5$	$a = 2.8$	$a = 3.1$	PNA +	PNA –	
$C_M$ ( $\mu\text{F}/\text{cm}^2$ )	$0.83 \pm 0.02$	$0.76 \pm 0.05$	$0.81 \pm 0.03$	$0.73 \pm 0.02$	$0.75 \pm 0.01$	$0.93 \pm 0.03$
$G_A$ ( $\text{mS}/\text{cm}^2$ )	$4.7 \pm 0.4$	$5.5 \pm 1.1$	$10.0 \pm 3.5$	$4.9 \pm 1.6$	$7.0 \pm 1.4$	$17 \pm 2$

TABLE III

Membrane capacity ( $C_M$ ) and apparent conductivity ( $G_A$ ) of mitogen-stimulated T and B cells and of control thymocytes

Cells from either spleen or lymph node were measured after 3 days stimulation with either concanavalin A (Con A, effective on T cells) or with lipopolysaccharide (LPS, effective on B cells). After 72 h, stimulated cells were identified in the rotation chamber by their larger size (radius  $4.4 \mu\text{m}$  instead of  $2.8 \mu\text{m}$ ). Thymocytes were incubated in the absence of mitogen. Most data are means  $\pm$  S.D. from four determinations, except for those in the last column which are the means and deviations of just three. In each determination 40–50 cells of each group were measured.

	Spleen cells		Lymph node cells		Thymocytes (controls)	
	Con A ( $4 \mu\text{g}/\text{ml}$ )	LPS ( $10 \mu\text{g}/\text{ml}$ )	Con A ( $5 \mu\text{g}/\text{ml}$ )	LPS ( $10 \mu\text{g}/\text{ml}$ )	0 h	72 h
$C_M$ ( $\mu\text{F}/\text{cm}^2$ )	$1.42 \pm 0.09$	$1.68 \pm 0.07$	$1.38 \pm 0.17$	$1.60 \pm 0.04$	$0.83 \pm 0.02$	$0.83 \pm 0.03$
$G_A$ ( $\text{mS}/\text{cm}^2$ )	$19 \pm 7$	$9.8 \pm 2.9$	$23 \pm 6$	$11 \pm 3$	$4.7 \pm 0.4$	$9.7 \pm 1.6$

agree with the lowest  $K_S$  values obtained on cell-sized polystyrene particles [25].

#### (b) Effect of 72 h stimulation

After 3 days incubation with mitogens, many cells became stimulated, as judged by their increase in size. Stimulated cells, defined as being those with a radius of  $4.4 \mu\text{m}$  or more, were measured. The results (Table III) on spleen cells agree well with those from lymph node cells in the case of both B and T cells. T cells (identified by their response to Con A) showed an approximate doubling of the membrane capacity to  $1.4 \mu\text{F}/\text{cm}^2$ , whilst B cells (those that responded to LPS) also showed a large increase (from  $0.9 \mu\text{F}/\text{cm}^2$  to  $1.6$ – $1.7 \mu\text{F}/\text{cm}^2$ ). Thymic cells (100% T cells) showed no significant  $C_M$  change during 72 h incubation without mitogen.

There was a significant increase in  $G_A$  above that of unstimulated cells (from  $4.6$ – $10 \text{ mS}/\text{cm}^2$  to  $19$ – $23 \text{ mS}/\text{cm}^2$ ) in T cells. The control thymocytes showed a smaller increase (from  $4.6$  to  $9.7 \text{ mS}/\text{cm}^2$ ). On the other hand the  $G_A$  of B cells decreased from  $17 \text{ mS}/\text{cm}^2$  to  $10$ – $11 \text{ mS}/\text{cm}^2$  during stimulation. Eqn. 3 shows that the change in cell size (from  $2.8$  to  $4.4 \mu\text{m}$ ) can partly explain the B cell data. If it is assumed that the entire  $17 \text{ mS}/\text{cm}^2$  of the  $G_A$  of  $2.8 \mu\text{m}$  cells is due to surface conductance, then a value of  $K_S$  of  $0.68 \text{ nS}$  results. If this value remained constant as the cell grew to  $4.4 \mu\text{m}$ , then the corresponding value of  $G_A$  would be  $7 \text{ mS}/\text{cm}^2$ . It is therefore still necessary to postulate increases in

either  $K_S$  or in  $G_M$  (at least  $3$ – $4 \text{ mS}/\text{cm}^2$ ), in order to explain the  $G_A$  value of  $10$ – $11 \text{ mS}/\text{cm}^2$  of stimulated B cells. In the case of T cells such increases must be larger, because  $G_A$  increased on stimulation. Eqn. 3 shows that the basal value of  $5.5 \text{ mS}/\text{cm}^2$  (Table II) corresponds to a maximum  $K_S$  of  $0.22 \text{ nS}$  and so to a probable maximum contribution of  $2.3 \text{ mS}/\text{cm}^2$  to the  $G_A$  of  $4.4 \mu\text{m}$  T cells. Therefore the measured  $G_A$  values for stimulated T cells of  $19$  and  $23 \text{ mS}/\text{cm}^2$  must be supposed to correspond to stimulation-induced increases in real  $G_M$  of  $17$  to  $21 \text{ mS}/\text{cm}^2$ .

Another interpretation of the increase in T cell  $G_A$  is that only  $K_S$  increases during stimulation. However, the simultaneous size increase makes this improbable \* and electrophoretic data (see Discussion) suggest that  $K_S$  decreases.

#### (c) Time-course of changes in T cells over 72 h

The fact that significant changes in surface properties (Tables II and III above) were seen after 72 h

\* Eqn. 3 shows that the  $K_S$  of the stimulated cells would have to increase to  $2.1 \text{ nS}$  if it alone caused the increase in  $G_A$ . This increase by a factor of  $9$ – $10$  seems unlikely because no equivalent changes in electrophoretic mobility, which should be at least approximately proportional to  $K_S$ , have been reported during activation [2–4].

mitogenic treatment raised the question of the kinetics of the process. Therefore incubations with measurements every 24 h were performed. For this work only thymocytes were used because of the relative ease with

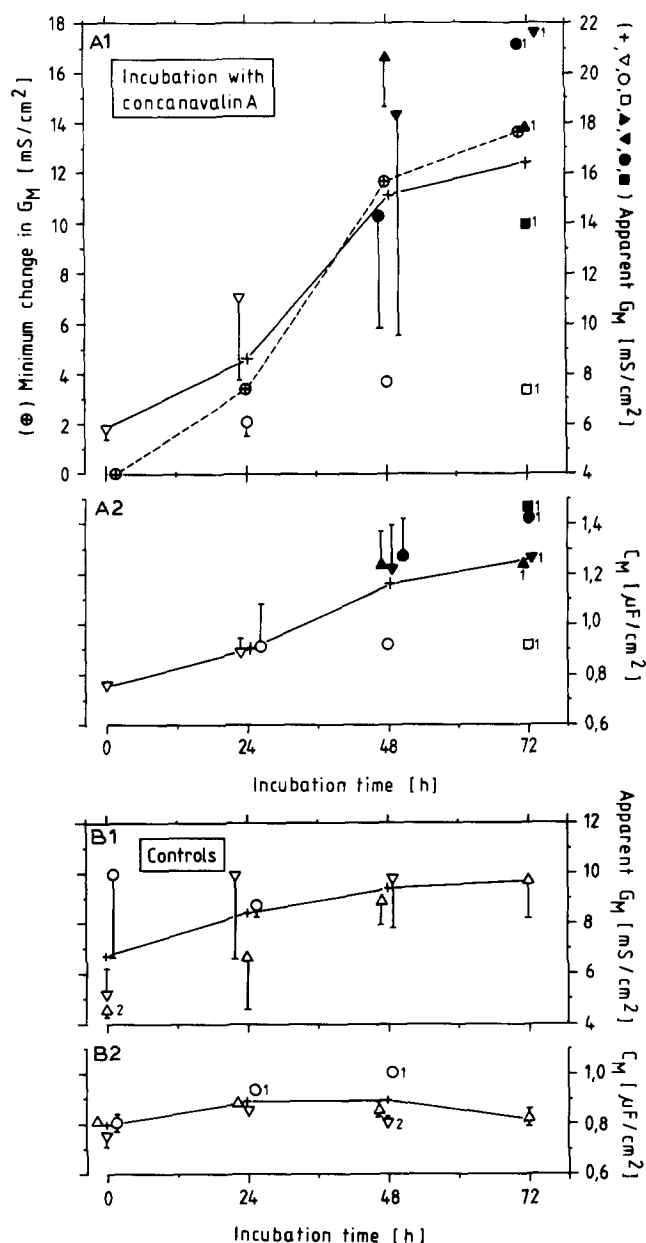


Fig. 4. The changes in the membrane properties of thymocytes during 3 days incubation with (A) and without (B) concanavalin A. The different symbols represent several size classes of cells given below. The lines connect the means of the  $G_M$  (A1 and B1) or  $C_M$  (A2 and B2) values for all sizes of cells: these mean values are shown by the symbol '+' except where this coincides with a size-class symbol. The data are means and standard deviations (where large enough to be shown) of three determinations except where the number of determinations appears. Each determination was as in Fig. 2 using at least 40 cells of each group. Cell radii were:  $\Delta$ , 2.5  $\mu\text{m}$ ;  $\nabla$ , 2.8  $\mu\text{m}$ ;  $\circ$ , 3.2  $\mu\text{m}$ ;  $\square$ , 3.5  $\mu\text{m}$ ;  $\blacktriangle$ , 3.8  $\mu\text{m}$ ;  $\blacktriangledown$ , 4.1  $\mu\text{m}$ ;  $\bullet$ , 4.4  $\mu\text{m}$ ;  $\blacksquare$ , 4.7  $\mu\text{m}$ . The diagrams for Con A-treated and control cells have axes of the same scale to allow direct comparison.

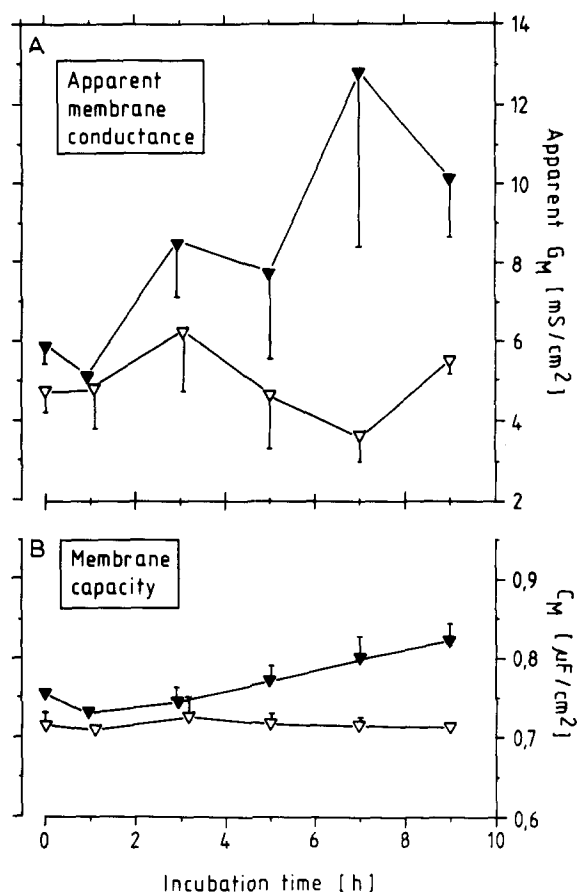


Fig. 5. The changes in the membrane properties of thymocytes during 9-h incubation with ( $\blacktriangledown$ ) and without ( $\triangledown$ ) concanavalin A. The data are means and standard deviations (where large enough to be shown) of 3 determinations. Each determination was as in Fig. 2 using at least 40 cells of each group. Note that 'apparent  $G_M$ ' or  $G_A$  is the sum of the effects due to  $G_M$  and  $K_S$  (see Eqns. 1 and 3).

which a pure preparation of such T cells could be obtained.

The upper part of Fig. 4 shows that the increases in  $C_M$  and in  $G_A$  occurred mainly between 24 and 48 h (see also Discussion). These trends are best seen from the mean values taken over all sizes of cells (shown as the interconnected '+' symbols). The other symbols represent particular sizes of cells (see legend to Fig. 4): it can be seen that the increases in  $C_M$  and  $G_A$  were strongly correlated with the size increases of the cells. The lower half of Fig. 4 shows that control cells showed little change in  $C_M$  but a small increase in  $G_A$  over the 72 h. These trends were the same whatever size of cell was measured, but larger cells (2.8 or 3.2  $\mu\text{m}$  radius, symbols ' $\nabla$ ' or ' $\circ$ ') initially showed higher values of  $G_A$  than did smaller cells (2.5  $\mu\text{m}$  radius, ' $\Delta$ ').

#### (d) Time-course of changes over 9 h

The experiments described above showed that part of the mitogen-induced changes in membrane parameters had occurred after only 24 h. It was of interest to

investigate how early during incubation changes were first detectable.

Measurements of cells (solid symbols in Fig. 5) at intervals of approximately 1 h showed that, after 5-h stimulation, definite increases in  $C_M$  and  $G_A$  above the starting values and above parallel controls were visible. Indeed an increase in  $G_A$  at 3 h may be discerned, at least above the starting value.

If the  $K_S$  is unaffected by stimulation, the increase in true  $G_M$  is equal to the difference in  $G_A$  values, because the cells remain of the same size during this period. An alternative interpretation of the  $G_A$  results is that the  $K_S$  doubles (from 0.19 nS or 0.22 nS to 0.44 nS) during the first 9 h stimulation. This could occur if the glycolyx became much thicker or more heavily charged.

## Discussion

### (a) The changes in capacitance

The values of  $C_M$  of unstimulated B and T lymphocytes ( $0.93 \mu\text{F}/\text{cm}^2$  and  $0.76 \mu\text{F}/\text{cm}^2$ , respectively) can be compared with those found using the suspension impedance technique. Fricke [26] obtained a value of  $0.91 \mu\text{F}/\text{cm}^2$  on a mixed rabbit leukocyte suspension. Asami et al. [6] have recently reported a  $C_M$  value of  $0.86 \mu\text{F}/\text{cm}^2$  in recent work on mouse splenocytes. The ratio between B and T lymphocytes in mouse spleen is between 1:1 and 7:3 [27], so that our  $C_M$  values lead to values for mixtures having these B:T ratios of  $0.845 \mu\text{F}/\text{cm}^2$  and  $0.88 \mu\text{F}/\text{cm}^2$ . The agreement between impedance and rotational values is therefore very good.

Rotation of T lymphocytes separated electrophoretically from human blood gave a  $C_M$  value of  $1.21 \pm 0.14 \mu\text{F}/\text{cm}^2$  (Arnold, W.M., Bauer, J., Hannig, K. and Zimmermann, U., unpublished). This higher value suggests differences between lymphocytes of different species or different degrees of maturation.

There appear to be no impedance data on the consequences of lymphocyte stimulation. Earlier rotation work [16] showed in-vivo stimulated, antibody-secreting mouse B cells to have higher  $f_c$  values than resting lymphocytes. On the basis of the present results this can be explained as being due to a large increase in  $G_A$ . Ziervogel et al. [17] also found increases in  $f_c$  upon mitogenic stimulation of lymphocytes from human blood. These were interpreted as large increases in membrane conductivity (the influence of  $K_S$  was not considered). Detailed data from analytical solutions for the membrane properties were not possible in Ref. 17 because a strong influence from the nuclear membrane was suspected. This was not the case here because we used much lower measurement frequencies (10–30 kHz instead of 250 kHz, see the discussion in Materials and Methods (d) of Fig. 1). Another reason why no effect from the nucleus is expected here is the very high conductivity ( $15 \text{ S}/\text{cm}^2$ ) of the nuclear membrane of

the mouse lymphocyte [6]. This will effectively short circuit the nuclear membrane at frequencies up to 3.5 MHz, so that it has little effect at the much lower frequencies (less than 50 kHz) used here.

The  $C_M$  values ( $1.5 \pm 0.2 \mu\text{F}/\text{cm}^2$ ) that we found for stimulated cells are higher than reported from impedance or rotation measurements on the majority of cells. However, this may be an apparent value caused by increase of the actual plasma-membrane area above that of a smooth sphere. This also explains the values of  $1.5 \mu\text{F}/\text{cm}^2$  and higher found in rabbit oocytes [11] and cultured insect ova cells [12,13]. This explanation is consistent with the slightly greater  $C_M$  of B cells compared to T cells ( $0.93 \mu\text{F}/\text{cm}^2$  compared to  $0.76 \mu\text{F}/\text{cm}^2$ ), because B cells are observed to have considerably more microvilli than T cells [28,29].

In the case of rabbit oocytes, the apparent  $C_M$  roughly doubled on fertilisation, consistent with electron microscopic studies of fertilisation [11], and  $G_M$  also increased. In guinea-pig lymphocytes [30], increases in membrane area upon stimulation have been seen in scanning electronmicrographs. Stimulation led to a dramatic increase in membrane folding. In a later study [29], 72 h incubation with Con A was shown to cause 96% of human lymphocytes to have multiple slender microvilli, not present in unstimulated T cells. These studies support the idea that changes in membrane area are the main cause of the increases in effective  $C_M$ . Changes in thickness or composition of the membrane are not required.

### (b) Conductance changes: relationship to electrophoretic data

There appear to be no other data on the 'high-frequency' conductivity of lymphocytes: suspension impedance work (see, for example, Ref. 6) has used media of such high conductivity that the low conductivity of the plasma membrane is unmeasurable. However, in low-conductivity media (as here), an apparent value ( $G_A$ ) of the membrane conductivity ( $G_M$ ) can be derived. As expressed by Eqns. 1 and 3 (Materials and Methods),  $G_A$  includes a contribution from the surface conductance  $K_S$ .

$G_A$  increases due to stimulation were observed particularly strongly in T cells. Arguments based on Eqn. 3 and the increase in cell size during stimulation make it likely that  $G_M$  dominates the change. This is consistent with the observation that Con A stimulation of Balb/c splenocytes gives rise to an increase in cation transport [31]. Presumably the increase in  $G_M$  upon activation reflects an increase in activity of pump proteins. The first detectable increase in ion transport occurred after 6 h stimulation [31]. This correlates well with the first definite increase in  $G_A$ , which was seen after 5 h stimulation. An increase in  $G_M$  also agrees with the 1.9-fold increase in the  $\text{K}^+$ -current of human peripheral T



lymphocytes noted after 20 h treatment with Con A [32].

The contributions from  $G_M$  and  $K_S$  can possibly be distinguished by comparison with results from cellular electrophoresis. As discussed in Materials and Methods (f), it is likely that cells with higher electrophoretic mobility have higher  $K_S$ . We now discuss three cases where this tentative link may apply.

(1) We found a higher apparent membrane conductivity ( $G_A$ ) in PNA-negative thymocytes than in PNA-agglutinatable cells. It is known that PNA-negative cells have higher electrophoretic mobility [33] due to their higher content of sialic acid, which masks the PNA binding site [34]. The larger  $G_A$  of PNA-negative cells may therefore be a sialic-acid mediated increase in  $K_S$ .

(2) Electrophoretic studies have shown [35] that mitogenic stimulation of T cells in a mixed lymphocyte population (as here) gives rise to larger cells with a decreased mobility (in contrast to those stimulated *in vivo*). This means that *in vitro* stimulation of T cells results in a decrease of their surface charge, which should decrease their  $K_S$ . This means that our values for the increase in  $G_M$  of T cells during stimulation are actually conservative, although the difference is small.

(3) The electrophoretic mobility of human peripheral B lymphocytes that are actively secreting antibodies is higher than that of resting cells [4]. The  $K_S$  of active cells, and therefore the  $f_c$  value, should also be above that of 'resting' B cells. This was observed in earlier rotational measurements on lymphocytes [16].

#### (c) Estimation of whole-cell data

It is possible to calculate values for the capacitance and conductance of whole cells from cell radii and the area-specific parameters yielded by rotation. The increase in membrane capacity of the T cells from  $0.76 \mu\text{F}/\text{cm}^2$  to  $1.24\text{--}1.26 \mu\text{F}/\text{cm}^2$  and the parallel increase in membrane conductivity occur whilst the cells are increasing in size. This means that the increases in membrane capacitance and conductance *per cell* are even larger, because stimulation causes an increase in radius and these quantities depend on membrane area:

$$C_{\text{cell}} = 4\pi \cdot a^2 \cdot C_M \quad G_{\text{cell}} = 4\pi \cdot a^2 \cdot G_M \quad (4)$$

As in the case of  $C_M$  and  $G_M$ ,  $C_{\text{cell}}$  and  $G_{\text{cell}}$  are parameters that express the sum of all effects that contribute to membrane capacitance and conductance. They are high-frequency measurements of the quantities measured by micro-electrode measurements or whole-cell patches [32,36]. Increases in rotational  $G_{\text{cell}}$  of between 4 and 40 nS occur after 24–72 h stimulation of thymocytes. These are comparable to the increase (approximately 5 nS) in cell conductance seen after 20 h stimulation of human peripheral T lymphocytes [32]. This voltage-gated [32,36]  $\text{K}^+$ -conductance was ob-

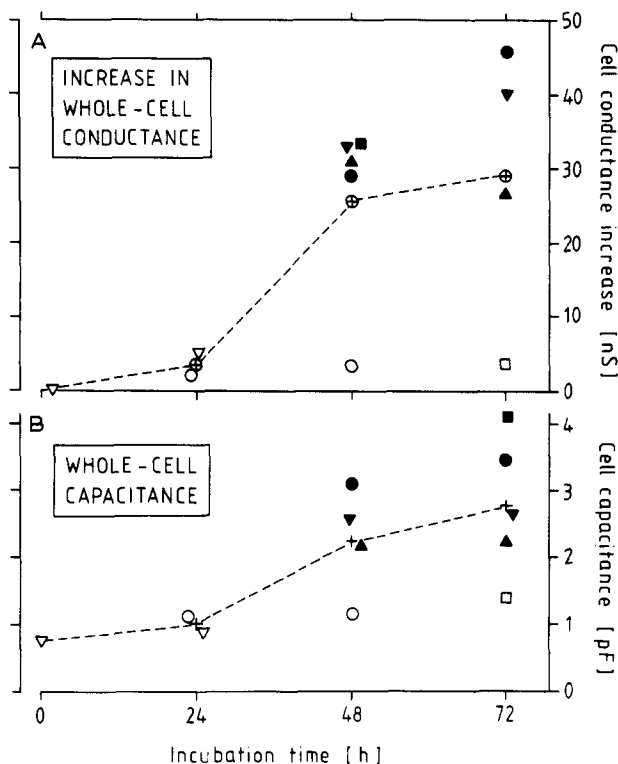


Fig. 6. Calculated changes in the total ('whole cell') membrane capacitance and conductance of thymocytes during 3 days incubation with concanavalin A. The values of conductance increase are the product of spherical cell area ( $4\pi \cdot a^2$ ) with  $G_M$  values obtained after subtraction of the maximum possible  $K_S$  contribution consistent with control cell data (as for the left-hand axis of Fig. 4). Hence these conductance changes are the minimum that can be deduced from the experimental data. The lines connect the means of the  $C_M$  or  $G_M$  values for all sizes of cells (the mean values are shown by the symbols + or  $\oplus$ , respectively). Symbols and other details as Fig. 4.

served by patch-clamp, so may be smaller than the high-frequency value from rotation \*.

Calculated values of  $C_{\text{cell}}$  and of the maximum change in  $G_{\text{cell}}$  (assuming no change in  $K_S$ ) are shown in Fig. 6. The vast majority of the increase in conductance occurs during the second day of stimulation. If it is assumed that the membrane remains unchanged in thickness and permittivity, then  $C_{\text{cell}}$  is directly proportional to membrane area. This means that the area of plasma membrane increases by a factor up to 5 ( $C_{\text{cell}}$  changes from  $0.76 \text{ pF}$  to between  $1.4 \text{ pF}$  and  $4.1 \text{ pF}$ , see Fig. 6) during 72 h activation. These data may be of interest in studies of membrane synthesis and turnover.

#### Conclusion

Electro-rotation can yield information on those surface properties of cells that are likely to alter during

\* Passive conductances are measured here, not voltage-induced ones. In addition, if the membrane properties are frequency-dependent, the high frequencies used in electro-rotation may result in lower values for  $C_M$  and higher values for  $G_M$  than those measured using micro-electrodes [9,11].

activation. Such properties are membrane capacity ( $C_M$ ) which indicates the degree of membrane ramification (folding and microvilli); membrane conductivity ( $G_M$ ) which is probably an indicator of membrane transport activity; and surface conductance ( $K_S$ ) which is an indicator of the extent and charge of the glycocalix. Separation of the contributions from  $K_S$  and  $G_M$  is only possible to a limited extent, but correlation with electrophoretic data may help.

Examination of lymphocytes at the single cell level has confirmed that the above properties change during mitogenic stimulation. The single-cell technique is particularly suited to this system because stimulated cells can be examined directly without interference from non-stimulated cells, otherwise a problem when measuring mixed suspensions. The onset of surface changes can be detected after 3–5 h stimulation, long before the cells increase in size, and at the same stage or earlier than changes in ion transport have been reported. It appears that an increase in membrane ramification is part of the activation sequence in these cells, as also seen after oocyte fertilisation [11]. The ability of electro-rotation to yield useful results with relatively few cells suggests its further application in the immunological field. In particular, it may be possible to examine how activation of cells *in vivo* differs from that *in vitro*.

**Note added in proof:** (Received 6 December 1989)

Recent calculations (Arnold, W.M. (1989) unpublished) show that a correction (due to neglect of the medium permittivity) is necessary to Eqn. 1: the change is negligible except for very small cells. It can be shown that  $C_M$  values from Eqn. 1 are too high by an amount  $2\epsilon_1/a$  where  $\epsilon_1$  is the absolute permittivity of the medium (80·88·54 fF/cm for aqueous media) and  $a$  the cell radius. Therefore, the  $C_M$  values quoted for stimulated lymphocytes (of radius 4.4  $\mu\text{m}$ ) must be decreased by 0.03  $\mu\text{F}/\text{cm}^2$ , whilst the values for control lymphocytes (radius 2.8  $\mu\text{m}$ ) must be decreased by 0.05  $\mu\text{F}/\text{cm}^2$ . There is no effect on  $G_M$  or  $K_S$  values. These slight corrections (2 to 6%) do not affect the interpretation of the results.

## Acknowledgements

We wish to thank Ms. S. Klüpfel for graphical assistance and Mr. U. Rimmel and Mr. A. Gessner for construction of rotation apparatus and chambers. This work was supported by a grant of the DFG to U.Z. and W.M.A. (SFB 176/B5) and by the Fonds der Chemischen Industrie to U.Z.

## References

- Andersson, J., Möller, G. and Sjöberg, O. (1972) *Cell. Immunol.* 4, 381–393.
- Hannig, K. and Heidrich, H.-G. (1989) *Free-flow Electrophoresis*, in press.
- Hückel, C., Brock, J., Rychly, J., Schulz, U., Kusnierczyk, P. and Paitasz, E. (1985) in *Cell Electrophoresis* (Schütt, W. and Klinkmann, H., eds.), pp. 669–676, De Gruyter, Berlin.
- Bauer, J., Kachel, V. and Hannig, K. (1988) *Cell. Immunol.* 111, 354–364.
- Gelfand, E.W., Cheung, R.K. and Grinstein, S. (1984) *J. Cell. Physiol.* 121, 533–539.
- Asami, K., Takahashi, Y. and Takashima, S. (1989) *Biochim. Biophys. Acta* 1010, 49–55.
- Pethig, R. (1979) *Dielectric and Electronic Properties of Biological Materials*, John Wiley and Sons, Chichester.
- Price, J.A.R., Burt, J.P.H. and Pethig, R. (1988) *Biochim. Biophys. Acta* 964, 221–230.
- Arnold, W.M. and Zimmermann, U. (1988) *J. Electrostat.* 21, 151–191.
- Arnold, W.M., Schmutzler, R.K., Schmutzler, A.G., Van der Ven, H., Al-Hasani, S., Krebs, D. and Zimmermann, U. (1987) *Biochim. Biophys. Acta* 905, 454–464.
- Arnold, W.M., Schmutzler, R.K., Al-Hasani, S., Krebs, D. and Zimmermann, U. (1989) *Biochim. Biophys. Acta* 979, 142–146.
- Freitag, R., Arnold, W.M., Zimmermann, U. and Schügerl, K. (1988) *Chem. Ing. Technik* 60, 1068–1069.
- Freitag, R., Arnold, W.M., Zimmermann, U. and Schügerl, K. (1989) *J. Biotechnol.* 11, 325–336.
- Glaser, R. and Fuhr, G. (1986) in *Electric Double Layers in Biology* (Blank, M., ed.), pp. 227–242, Plenum Press, New York.
- Schwan, H.P. (1988) *Ferroelectrics* 86, 205–223.
- Arnold, W.M. and Zimmermann, U. (1985) German patent DE 33 23 415 C2, Verwendung eines Verfahrens und einer Vorrichtung zur Bestimmung von Zellinhaltsstoffen sezernierenden Zellen. Applied for 29 June 1983, published 10 Jan 1985. Also European patent 0 130 530 B1, applied for 26 June 1984, granted 24 June 1987.
- Ziervogel, H., Glaser, R., Schadow, D. and Heymann, S. (1986) *Biosci. Rep.* 6, 973–982.
- Reisner, Y., David, A. and Sharon, N. (1976) *Biochem. Biophys. Res. Commun.* 72, 1585–1591.
- Reisner, Y., Linker-Israeli, M. and Sharon, N. (1976) *Cell. Immunol.* 25, 129–143.
- Arnold, W.M. and Zimmermann, U. (1985) German patent DE 33 25 843 C2, Verfahren und Vorrichtung zur Unterscheidung von in einem Medium befindlichen Partikeln. Applied for 18 August 1983, published 7 Feb. 1985. Also: European patent 0 131 944, applied for 16 July 1984, granted 25 May 1988.
- Arnold, W.M. (1988) *Ferroelectrics* 86, 225–244.
- Arnold, W.M. and Zimmermann, U. (1982) *Z. Naturforsch.* 37c, 908–915.
- Schwan, H.P. (1985) *Stud. Biophys.* 110, 13–18.
- Gimsa, J., Fuhr, G. and Glaser, R. (1985) *Stud. Biophys.* 109, 5–14.
- Arnold, W.M., Schwan, H.P. and Zimmermann, U. (1987) *J. Phys. Chem.* 91, 5093–5098.
- Fricke, H. (1953) *Nature* 172, 731–732.
- North, R.T. (1974) in *Mechanisms of Cell-Mediated Immunity* (McCluskey, R.T. and Cohen, S., eds.), pp. 185–220, Wiley, New York.
- Polliack, A., Lampen, N., Clarkson, B.D. and De Harven, E. (1973) *J. Exp. Med.* 138, 607–624.
- Polliack, A., Touraine, J.-L., De Harven, E., Lampen, N. and Hadden, J.W. (1975) *Isr. J. Med. Sci.* 11, 1285–1298.
- Robineaux, R., Orme, W. and Orme-Rosselli, L. (1969) *Compt. Rend. Acad. Sci. Paris D* 268, 2139–2142.
- Owens, T. and Kaplan, J.G. (1980) *Can. J. Biochem.* 58, 831–839.
- Matteson, D.R. and Deutsch, C. (1984) *Nature* 307, 468–471.
- Rychly, J. and Ziska, P. (1985) in: *Cell Electrophoresis* (Schütt, W. and Klinkmann, H., eds.), pp. 681–690, De Gruyter, Berlin.
- Despont, J.P., Abel, C.A. and Grey, H.M. (1975) *Cell. Immunol.* 17, 487–494.
- Galili, U., Häyry, P. and Klein, E. (1979) *Cell Immunol.* 48, 91–99.
- DeCoursey, T.E., Chandy, K.G., Gupta, S. and Cahalan, M.D. (1984) *Nature* 307, 465–468.